Chapter 14

Modeling in situ iron removal from groundwater with trace elements such as As

C.A.J. Appelo[1] and W.W.J.M. de Vet[2]
[1]Hydrochemical Consultant, Valeriusstraat 11
1071 MB Amsterdam, The Netherlands
[2]Hydron-ZH, Postbus 122, 2800 AC Gouda, The Netherlands

The cyclic injection of oxygenated water in an aquifer may induce in situ iron removal from groundwater. During injection of aerated water, sorbed ferrous iron is displaced by cations, oxidized in the pore space, and precipitated as ferric iron oxyhydroxide. During pumping, ferrous iron is sorbed from groundwater on the exchange and sorption sites, and the breakthrough of dissolved iron is retarded. Other trace elements such as arsenic may be eliminated jointly with iron by sorption or co-precipitation.

The volume of iron-free groundwater that can be pumped per volume of injected, aerated water defines the efficiency of the process. The efficiency is determined by the ratio of the retardations of oxygen during injection and of iron during pumping. This chapter shows how these retardations can be calculated for given water qualities and aquifer compositions.

The first seven cycles of an in situ iron removal project in The Netherlands were simulated with the hydrogeochemical transport model PHREEQC (version 2). The concentration changes of CH_4, NH_4^+, Mn^{2+}, Fe^{2+}, PO_4^{3-} and As are discussed in detail. Arsenic shows concentration jumps in pumped groundwater which are related to oxidation/reduction and sorption/desorption reactions resulting from the water quality variations.

1. INTRODUCTION

In situ iron removal is a useful technique for reducing the iron concentration in groundwater pumped for consumption or industrial purposes (Hallberg and Martinell, 1976; Meyerhoff, 1996; Rott and Lamberth, 1993; Van Beek, 1980). The technique entails the periodic injection of a volume of aerated or oxygenated water in an aquifer, followed

by pumping of the injected water and subsequently of groundwater in which the iron concentration is lower than in native groundwater. Iron in the aquifer is oxidized during injection of the oxygenated water and precipitates as iron-oxyhydroxide. The loss of iron also liberates cation exchangers which are filled again when pumping is resumed and groundwater with dissolved iron contacts the cation exchange sites in the aquifer (Appelo et al., 1999). The precipitated iron forms a sorber which augments the exchange capacity of the aquifer. Moreover, iron-oxyhydroxide is a well known scavenger for heavy metals, and by analogy with above ground operations (Benjamin et al., 1996) it can be expected that together with iron, the concentrations of heavy metals in groundwater will decrease as well. A loss of arsenic with in situ iron removal has been reported already (Rott et al., 1996).

However, it is still fairly uncertain which chemical or biochemical process takes the lead in changing the concentrations of heavy metals in aquifers. Sorption on ferrihydrite can now be modeled in great detail using data from laboratory experiments, but to discern between sorption and desorption and uptake and release in a growing and reordering precipitate is difficult even in the laboratory (Eick et al., 1999; Fuller et al., 1993; Gerth et al., 1993; McKenzie, 1980; Nesbitt et al., 1995; Waychunas et al., 1993; Zachara et al., 1987). It is also clear that other iron-oxyhydroxides than ferrihydrite exhibit other sorption behavior, and have other constants in the surface complexation model (Mathur, 1995). Another drawback is that complexation constants for Fe^{2+} and HCO_3^- are lacking, although these are important species in groundwater that will influence sorption of other elements. Thus, it is important to perform field studies which show the applicability of our models for sorption in natural systems (Davis et al., 1998; Kent et al., 2000; Runkel et al., 1999; Stollenwerk, 1998) and this chapter follows that line.

In particular, data were interpreted from the groundwater pumping station Schuwacht of Hydron-ZH (Gouda, The Netherlands) where the water quality was monitored for the first 7 cycles of in situ iron removal. Emphasis was placed on the effects for arsenic concentrations, prompted by fear that the subsoil might become contaminated by trace elements which are incorporated in the iron precipitates. The general principles of in situ iron removal are not difficult and the efficiency of the operation can be estimated with simple formulas. However, for arsenic also redox effects and complicated displacements from sorption sites are significant which cannot be calculated without numerical models. This chapter describes the general principles of in situ iron removal and discusses details of the Schuwacht plant starting with simple hand calculations for basic insight and continuing with more comprehensive modeling for As.

2.   PRINCIPLES OF IN SITU IRON REMOVAL

Concentration profiles of oxygen and iron at three successive steps of in situ iron removal are shown in Figure 1. During injection of 1000 m^3 aerated water, groundwater with dissolved iron is displaced in the aquifer. If sorption sites would be absent, ferrous iron would simply move along with groundwater, and the reaction between oxygen and Fe^{2+} would be limited to small amounts due to mixing at the front. However, cations from injected water exchange for sorbed Fe^{2+} and the oxidation of this iron consumes oxygen. Thus, the oxygen front lags behind the injection water front. When the operation is switched to pumping, first the injected volume is withdrawn, with some front spreading as result of dispersion. Then, for some time, groundwater can be pumped with a reduced iron concentration, because ferrous iron is lost to the exchange sites as groundwater flows through the oxidized zone. After a fixed time, or when the iron concentration passes some limit, another volume of aerated water is injected and the next cycle (or run) of in-situ iron removal begins.

The efficiency of the process can be calculated if we neglect dispersion and limit the sorption reactions to the zone where oxygen has penetrated, and then consider how much iron can be sorbed in that part of the aquifer. Thus, first the position of the oxygen front at the end of the injection stage must be located. This position can be found from the reaction of oxygen with ferrous iron:

$$O_2 + 4Fe^{2+} + 4H^+ = 2H_2O + 4Fe^{3+} \tag{1}$$

All dissolved Fe^{2+} for this reaction comes from sorbed iron and the retardation of oxygen amounts to:

$$R_{O_2} = 1 + q_{Fe}/4m_{O_2} \tag{2}$$

where q_{Fe} is sorbed iron (mol/l pore water) and m_{O_2} is dissolved oxygen in injection water (mol/l). Sorbed iron in eqn. 2 is in exchange equilibrium with dissolved iron in groundwater and can be calculated with standard geochemical programs as will be demonstrated in section 3.

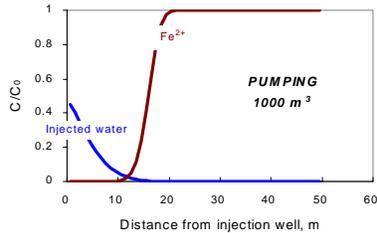Water with oxygen is injected in a reduced aquifer.

Fe^{2+} is exchanged from exchange complex and dissolves in injected water.

Oxygen lags behind injection front as it reacts with Fe^{2+}. Oxidized Fe^{3+} precipitates.
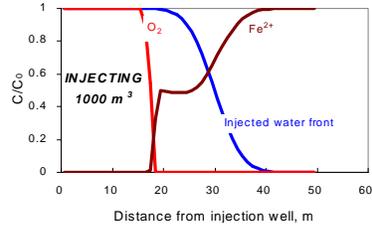
Injected water is withdrawn.

Solute Fe^{2+} is sorbed on exchanger when groundwater is pumped.

GROUNDWATER WITHOUT IRON CAN BE PUMPED

Efficiency depends on local conditions: oxidant amount in injected water **and** exchange capacity of the aquifer.
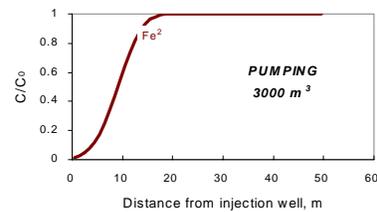
Figure 1. Oxygen- and iron-concentration profiles at three stages of an in-situ iron removal cycle.

For the case of linear flow, the distance between the oxygen front and the injection well is:

$$x_{O_2} = x_{inj} / R_{O_2} \tag{3}$$

where x_{inj} is the distance traveled by the injected water. The fraction of injected water from which oxygen is activily utilized in the process is:

$$f_{inj} = (x_{inj} - x_{O_2}) / x_{inj} = 1 - 1/R_{O_2} \tag{4}$$

Note that eqn. 4 implies that oxygen may not be reacting at all when the retardation equals 1, *i.e.* when sorbed iron is zero, or $q_{Fe} = 0$ in eqn. 2. On the other hand, all oxygen is used when sorbed iron is infinite. Thus, the efficiency of in situ iron removal depends on the sorption capacity of the aquifer for iron, and it will be low in a coarse, gravelly aquifer.

Now during pumping, if native groundwater with dissolved iron returns and flows along the emptied sorption sites, Fe^{2+} will be sorbing again, and iron is retarded with respect to groundwater flow. The retardation equals:

$$R_{Fe} = 1 + q_{Fe}/m_{Fe} \qquad (5)$$

Equation (5) allows to calculate the volume of groundwater that can be pumped until the sorption sites are all filled again and the iron concentration of native groundwater arrives at the well. The volume of water in between the injection well and x_{O_2} is:

$$V_{inj}\,(1 - f_{inj}) = V_{inj}\,/\,R_{O_2} \qquad (6)$$

And the volume of groundwater which can be pumped is:

$$V_{gw} = V_{inj} \times R_{Fe}\,/\,R_{O_2} \qquad (7)$$

Note again, that eqn. 7 implies that iron arrives immediately at the well when the ratio of sorbed and dissolved iron is very small, and, of course, that it will never arrive when the concentration of dissolved iron is zero. Thus, the efficiency of in situ iron removal also depends on the concentration of iron in groundwater.

We can define the efficiency of in situ iron removal as:

$$E = V_{gw}\,/\,V_{inj} \qquad (8)$$

which, according to eqn. 7, equals:

$$E = R_{Fe}\,/\,R_{O_2} \qquad (9)$$

For a hand calculation, we may assume that q_{Fe} in eqn. 5 is the same as was used for calculating the reaction of oxygen in eqn. 2, and initially neglect the additional sorption of iron on the precipitate. Otherwise, if the sorption on the precipitated iron-oxyhydroxide is known, it can be used to increase q_{Fe} in eqn. 5 with respect to eqn. 2 by the appropriate factor.

3. SORPTION REACTIONS OF Fe^{2+}

Sorption in aquifers takes place mainly on clay minerals, organic matter and oxides, and is differently modeled depending on the properties of the solid. Clay minerals such as smectite and illite carry a charge due to

structural substitutions which is constant at the pH's of groundwater. Sorption of cations is, in this case, a cation exchange reaction which does not affect the charge of the clay mineral. For example when Na^+ from injection water displaces Fe^{2+} from the exchange sites of the clay mineral, the reaction is:

$$Na^+ + Fe-X_2 = Na-X + Fe^{2+}; \quad \log K = -0.22 \qquad (10)$$
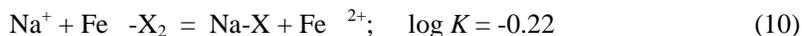
Here, X indicates the cation exchanger, with a charge of X^-. The cation exchange capacity (CEC, $mmol_c/kg$) can be estimated with empirical formulas such as:

$$CEC \ (mmol_c/kg) = 7 \cdot (\% \ clay) + 35 \cdot (\% \ C) \qquad (11)$$

where (% clay) and (% C) are the weight percentages of clay $< 2\mu m$ and organic carbon, respectively (Appelo and Postma, 1993). The CEC can be recalculated to a capacity per liter groundwater by multiplying with the bulk density ρ_b (kg/dm^3) and dividing by the water filled porosity ε_w (-):

$$X^- \ (mmol_c/l) = CEC \ (mmol_c/kg) \cdot \rho_b / \varepsilon_w \qquad (12).$$

Cation exchange in groundwater is a multicomponent process in which all the solute cations participate. It can be calculated easily with geochemical models such as PHREEQC-2 (Parkhurst and Appelo, 1999) which have databases with representative values of the exchange constants. An example PHREEQC-2 input file for calculating exchangeable iron is given in Table 1.

Sorption to iron-oxyhydroxide can be computed with the surface complexation model of Dzombak and Morel (1990). This model assembles the results of numerous laboratory experiments on sorption of trace elements to ferrihydrite (Hfo, hydrous ferric oxide, FeOOH). Ferrihydrite is a more or less amorphous substance which is found in nature in seepage zones of reduced, iron containing groundwater. Probably, it will be representative for the iron-oxyhydroxide which forms during in situ iron removal in aquifers, but this has not been verified yet.

The main difference between surface complexation and exchange is that the surface complexer will acquire a charge depending on the ions which are sorbed to the surface. The proton is an important charge-determining ion, and in distilled water ferrihydrite will carry a charge depending on the pH and be chargeless at a pH of about 8.1. Thus, at pH = 7, ferrihydrite has a positive charge and cations are bound only when their chemical affinity to the surface oxygens is sufficient to overcome the electrostatic repulsion. The

Table 1. PHREEQC-2 input file for calculating exchangeable and sorbed iron, and the undimensional distribution coefficient for iron.

```
# Download PHREEQC-2 via links in www.xs4all.nl/~appt
# or directly from www.geo.vu.nl/users/posv/phreeqc.html
# or wwwbrr.cr.usgs.gov/projects/GWC_coupled/phreeqc/index.html

# Part A: define iron oxide and groundwater composition
PHASES
 Ferrihydrite; FeOO2H3 + 3H+ = Fe+3 + 3H2O; log_k 2.0
EQUILIBRIUM_PHASES 1
 Ferrihydrite 0.0 32e-3     # 300 ppm Fe in sediment / 56 * 6
SOLUTION 1
 -units mg/l; -temp 10
 pH     7.1; pe   0.0 Ferrihydrite
 Na    77.3; K    5.3; Mg 13.1; Ca 93
 Amm    3.8; Fe   6.0; Mn  1.1
 Cl   134.0; S(6) 43.4; Alkalinity 308 as HCO3
 P      3.16   as PO4; As  10 ug/l
SAVE solution 1
END

# Part B: define exchangeable and sorbed iron
USE solution 1
EXCHANGE 1
 -equil 1; X 0.03     # fine sand, CEC = 5 mmolc/kg
SURFACE 1
 -equil 1; Hfo_w Ferrihydrite 0.2 5.3e4; Hfo_s Ferrihydrite 0.005
USER_PRINT
 10 Cplx_Fe = mol("Hfo_sOFe+") + mol("Hfo_wOFe+") + mol("Hfo_wOFeOH")
 20 print "FeX2 =", mol("FeX2"), " Fe on Hfo =", Cplx_Fe
 30 print " Kd  =", (mol("FeX2") + Cplx_Fe) / tot("Fe")
END
----------------------------------User print---------------------------
FeX2 =  1.8662e-04  Fe on Hfo =   5.2851e-04
 Kd  =  6.6517e+00
```

electrostatic effect is calculated with the Boltzmann factor, $\exp(-zF\psi/RT)$, where the potential ψ is a function of the charge and the surface area of the ferrihydrite, and, in Dzombak and Morel's model, of the ionic strength of the solution. Chemical binding is distributed over weak and strong sites which exist in a proportion of 0.2 and 0.005 mol sites / mol ferrihydrite. The increasing complexation capacity with increasing amounts of ferrihydrite that precipitate during in situ iron removal can be modeled with PHREEQC-2 by coupling Hfo, the moles of the surface complex, to the mass of ferrihydrite in the system, cf. Table 1.

Surface complexation is a typical multi-component reaction, similar to cation exchange. The database for surface complexation includes complexation constants for major elements in groundwater such as Ca^{2+} and SO_4^{2-}, but not for Fe^{2+} and HCO_3^-. In the first instance, constants for these ions can be estimated with linear free energy relations (*LFER*'s) in which the properties of similar chemical systems are compared and interpolated (Dzombak and Morel, 1990). Thus, the surface complexation constant for Fe^{2+} is expected to lie in between the ones for Cd^{2+} and for Zn^{2+}, in line with the known differences of the association constants of these heavy metals with OH^- in water. For the weak sites, the *LFER* gives:

$$Hfo\_wOH + Fe^{2+} = Hfo\_wOFe^+ + H^+; \qquad \log K = -2.5 \qquad (13)$$
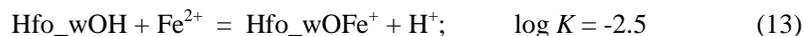
The *LFER*-derived complexation constant K enabled to fit the recently published experimental sorption isotherm of Liger et al. (1999) very well, except at pH > 8 (Fig. 2). The deviation at higher pH is due to sorption of a hydroxy complex and the data of Liger et al. were used for optimizing new constants for the database which are given in Table 2. The complexation constant for the strong sites could not be derived from Liger's data because the concentration was low for ferrihydrite and high for Fe^{2+}. The value in Table 2 was obtained from new measurements by C. Tournassat with more appropriate concentrations in the experiment. It may be noted that the experimental value is much different from the one which can be estimated by interpolation with Cd^{2+} and Zn^{2+}, thus indicating that the *LFER* value needs to be checked whenever possible.

Another important ion in groundwater, HCO_3^-, is also lacking from the database in Dzombak and Morel's model. The bicarbonate ion is usually avoided in sorption experiments with oxides because of pH buffering and slow, kinetic exchange at the air-solution interface. The experimental data of Van Geen et al. (1994) for goethite were used to derive complexation constants for ferrihydrite which are listed in Table 2. Although goethite has a much higher crystallinity than ferrihydrite, it was found that the sorption envelope of HCO_3^- on ferrihydrite measured by Zachara et al. (1987) could be modeled with nearly the same constants (Appelo et al., 2002). The major effect of sorption of HCO_3^- on ferrihydrite is identical to what was noted already by Van Geen et al. for goethite, *i.e.* a large proportion of the surface sites will be occupied by HCO_3^- at the usual bicarbonate concentrations in groundwater.
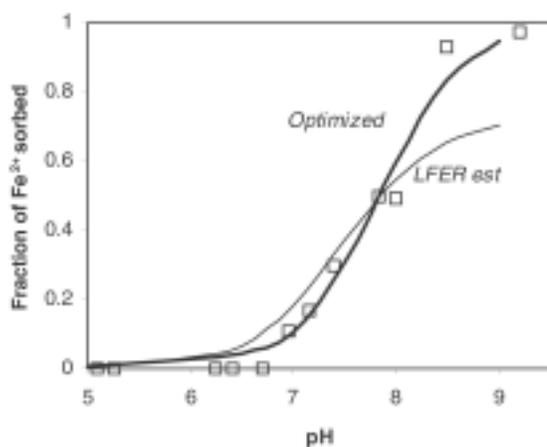
Figure 2. Sorption edge of Fe^{2+} on ferrihydrite, data from Liger et al. (1999), model with surface complexation constants estimated from linear free energy relation (LFER) and model optimized on the data of Liger et al.

Table 2. Surface complexation constants of Fe^{2+} and HCO$_3^-$ on ferrihydrite (Appelo et al., 2002).

Hfo_wOH + CO$_3^{2-}$ + H$^+$ = Hfo_wOCO$_2^-$ + H$_2$O	log K 12.56[1]
Hfo_wOH + CO$_3^{2-}$ + 2H$^+$ = Hfo_wOCO$_2$H + H$_2$O	log K 20.62[1]
Hfo_wOH + Fe^{2+} = Hfo_wOFe$^+$ + H$^+$	log K = -2.98[2]
Hfo_wOH + Fe^{2+} + H$_2$O = Hfo_wOFeOH + 2H$^+$	log K = -11.55[2]
Hfo_sOH + Fe^{2+} = Hfo_sOFe$^+$ + H	log K = -0.95[3]

[1]Optimized using data from Van Geen et al. (1994), slightly different in Appelo et al. (2002)
[2]Optimized using data from Liger et al. (1999)
[3]Optimized using data from C. Tournassat

4.   A SPECIFIC EXAMPLE: PUMPING STATION SCHUWACHT, HYDRON-ZH

Pumping station Schuwacht of the drinking water company Hydron-ZH is a bank filtration unit with the pumping wells located at a distance of 70 - 200 m from the river Rhine near Gouda, The Netherlands. In 1998 and 1999, pumping from filter PP8 was periodically interrupted to inject a volume of treated and aerated groundwater. Water was injected at 30 m^3/h for 2 days

and immediately afterwards pumping was resumed at 23 m^3/h for 40 days. The purpose of the injection was to ameliorate the conditioning of the raw water for the water treatment plant where iron, manganese, ammonia and methane are removed.

Pumping well PP8 is located in coarse sandy sediments of the Sterksel formation at a depth of 20-30 m bs. Chemical analysis of the sand provided an average of 0.5% calcite, 0.03% organic carbon, 300 ppm Fe as Fe-oxide, no pyrite, and less than 1 ppm As. The lower 7 m sediment contained 1% silt, the upper 3 m 5-7% silt and the porosity was 0.34. The sediment's exchange capacity was estimated to be 5 mmol$_c$/l in the coarse sandy lower part and 30 mmol$_c$/l in the upper 3 m.

Water in the well originates for almost 100% from the Rhine, but the water quality has changed during infiltration in the riverbed and passage through the aquifer. The concentrations of Ca^{2+}, Fe^{2+}, Mn^{2+}, NH_4^+ and the alkalinity have increased, and the groundwater contains methane. Methane is important for judging the suitability of an aquifer for in situ iron removal and for modeling the chemical processes, since it often indicates a redox state in which sulfides have formed and are stable. When sulfides are present, a rapid reaction with injected oxygen will have various adverse effects for the water quality, varying from decrease of pH to increase of heavy metals. However, methane formation is not expected in the Sterksel aquifer for the given, low concentration of organic carbon, but it may originate in the organic rich layers of the riverbed. Water sampled at various times showed that the methane concentration was inversely coupled to the SO_4^{2-} concentration and increased linearly as the ratio of SO_4^{2-} to Cl^- decreased. This indicates that methane is probably formed locally during infiltration in the river bed in part of the water after SO_4^{2-} has been reduced, and that this water is mixed with water without methane but with SO_4^{2-} in the well. In this case, sulfides may be present in the riverbed, but they are not expected in the aquifer and need not be considered for the in situ iron removal operation. Water quality analyses are given in Table 3.

4.1   Efficiency calculations

The oxygen concentration in the injected water was 0.28 mmol O_2 / l. According to reaction 1, this amount can oxidize 1.12 mmol Fe^{2+} / l. The iron concentration in native groundwater is 0.1 mmol Fe^{2+} / l, and the simplest calculation would predict an efficiency of 11.2, *i.e.* for every liter of injected water, 11.2 liters groundwater without iron may be pumped. However, it was noted above (reaction 2) that the efficiency is limited by the intermediate reaction with sorbed iron.

The concentration of sorbed Fe^{2+} in the fine sandy part of the aquifer can be calculated to be $q_{Fe} = 0.19$ mmol/l for the initial groundwater quality (first analysis in Table 3). Using eqn. 2, the retardation of the oxygen front is $R_{O_2} = 1 + 0.19/(4 \times 0.28) = 1.17$. At the end of the first cycle, 1440 m^3 water were injected and the front had radiated to 11.8 m from the well, with 9.7 m filter length and porosity 0.34. The oxygen front was then located at the position which conforms to the injection of $1440/1.17 = 1230$ m^3, or 10.9 m. The fronts were also calculated with PHREEQC-2 (Parkhurst and Appelo, 1999) and are given for cycles 1 and 7 in Figure 3. The modeled oxygen front for the first run shows slightly more retardation than was calculated by hand, because injected water was oxidizing dissolved Fe^{2+} at the front by mixing with groundwater. Mixing by dispersion in the aquifer is included in the computer model, but the reactions due to this process are difficult to account for in hand calculations.
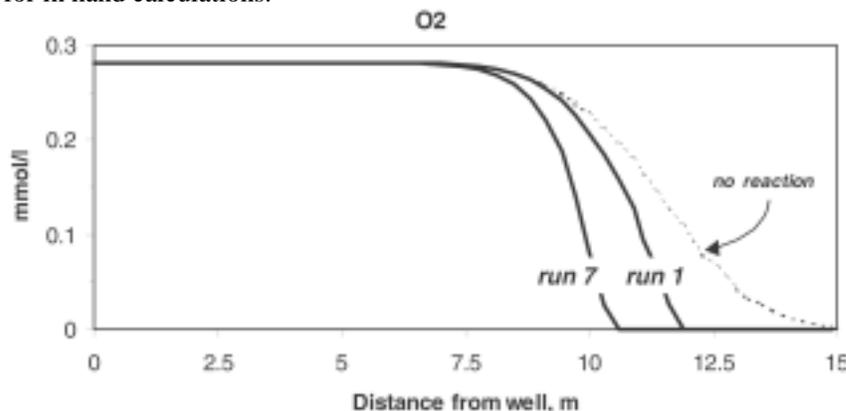

Figure 3. Calculated oxygen profiles at the end of the injection of aerated water in cycles 1 and 7 of in situ iron removal in Schuwacht.

During pumping, ferrous iron is sorbed to 0.19 mmol/l exchange sites, and furthermore to 0.19 mmol/l precipitated iron-oxyhydroxide. The amount sorbed to iron-oxyhydroxide was calculated to be 0.2 mol Fe^{2+} per mol iron-oxyhydroxide for the water composition of PP8 (discussed later). The total iron sorbed during the first cycle is thus $0.19 + (0.2 \times 0.19) = 0.23$ mmol/l. The expected efficiency is therefore, from eqn. 9, $E = R_{Fe}/R_{O_2} = (1 + 0.23/0.1) / 1.17 = 2.8$. Note that it is the dynamics of the system, expressed by the retardations of the ions, that makes the efficiency decrease to a much smaller value than was estimated earlier when assuming simply that all O_2 was available for oxidation of iron.

In the second run, sorbed iron had increased to $q_{Fe} = 0.23$ mmol/l, and therefore the oxygen front was more retarded than in the first cycle. Also,

0.23 mmol/l iron-oxyhydroxide precipitated and the sorption capacity amounted to $0.19 + (0.2 \times (0.19 + 0.23)) = 0.27$ mmol/l in the third run. The increased sorption capacity resulted in a more retarded O_2 front which is illustrated for the 7th run in Figure 3. The retardation and hence the efficiency will continue to increase until in the final end all oxygen is reacting immediately at the injection well, and the theoretical limit of 11.2 is reached for the efficiency.

4.2   Amounts and distribution of precipitate

The total amount of iron-oxyhydroxide which precipitated during a cycle in Schuwacht, can be estimated from:

$$[Fe(OH)_3]_n = (0.19 + 1.2 \times [Fe(OH)_3]_{n-1}) \tag{14}$$

where $[Fe(OH)_3]_n$ indicates mol precipitate/l at run number n. For run 7 the amount is 2.5 mmol $Fe(OH)_3$/l, or 23 ppm Fe in the sediment, which is in good agreement with the model calculation shown in Figure 4. The total precipitate after run 7 would occupy 0.009% of the porosity, assuming a density of 3.0 kg/dm^3 for the precipitate. The amounts are small and, indeed, clogging has not been observed in systems which have been operating for over 20 years (Meyerhoff, 1996). Clogging is probably also prevented because closing pores will force the injected water to pass around, thus evening out the reaction in space.
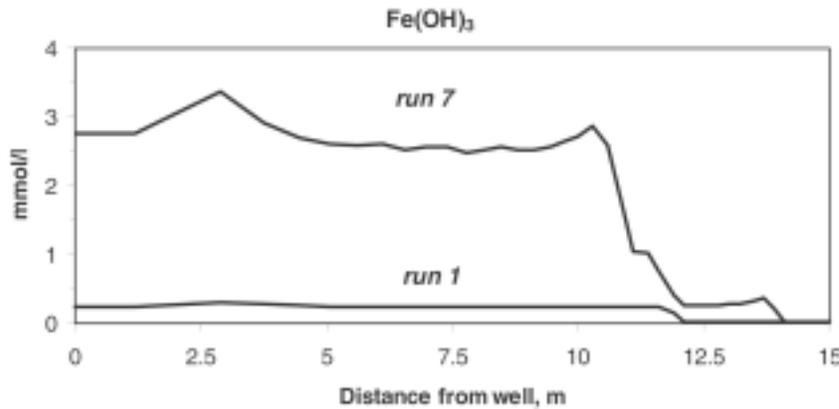

Figure 4. Calculated profiles of precipitated iron-oxyhydroxide in cycles 1 and 7 in Schuwacht.

4.3   Concentration fronts of selected elements during pumping

Cation exchange will modify the concentrations in groundwater during pumping of groundwater, and it will be different for cations which sorb on clay minerals (such as NH_4^+), and for ions which also sorb on iron-oxyhydroxide. Elements which do not sorb, will be a tracer for the groundwater front and it was found that methane behaved conservatively in Schuwacht. Equilibria with calcite, siderite and rhodochrosite were also considered in separate model runs, but the carbonates seemed to be unimportant in Schuwacht. Thus, the model results described here, are for a system with cation exchange and surface complexation only.

Methane

Figure 5 shows the methane concentration for cycles 1 and 7 as function of the ratio of pumped and injected volume, V/V_{inj}. The methane concentration was half of the groundwater concentration at $V/V_{inj} = 1$, and close to the final concentration at $V/V_{inj} = 2$. The end concentration was 2 mg CH_4/l in the first run, and 0.8 mg/l in the 7th run due to variations in the groundwater quality. However, the concentration patterns were identical in both runs, and conform to a conservative substance, with a dispersivity of 0.3 m of the aquifer. The concentrations of HCO_3^- and dissolved organic carbon also showed conservative behavior, which indicates that injected water did not react with sedimentary organic carbon.
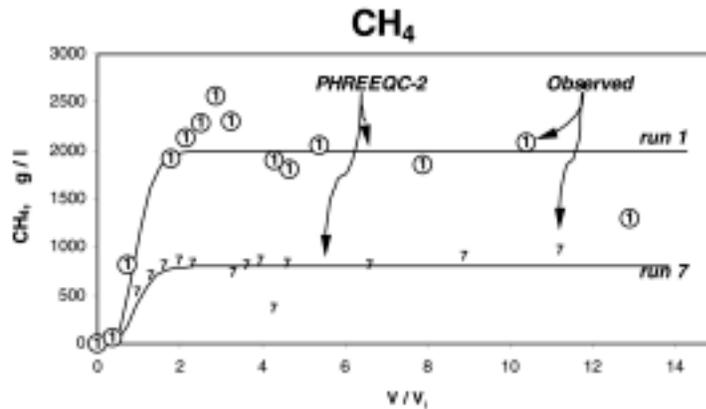

Figure 5. Observed and modeled methane concentrations in cyles 1 and 7 in Schuwacht.

Ammonium

Figure 6 shows the ammonium concentration for cycles 1 and 7. The groundwater concentration of ammonium changed from 3.8 in cycle 1 to 3.3 mg/l in cycle 7. Figure 6 shows a dotted line for conservative flow, and a full line for the case that cation exchange is included in the model. The insignificant difference is due to the small exchange capacity of 5 $mmol_c/l$ for the lower 7 m and 30 $mmol_c/l$ for the upper 3 m of the aquifer. The heterogeneity was modeled in separate computer runs for the upper and the lower part, adapting only the cation exchange capacity and combining the model results in the proportion of 3:7. The model results for runs 1 and 7 would coincide exactly when normalized to the final concentration, because the exchange capacity of the sediment is invariant and iron-oxyhydroxide does not adsorb ammonium.
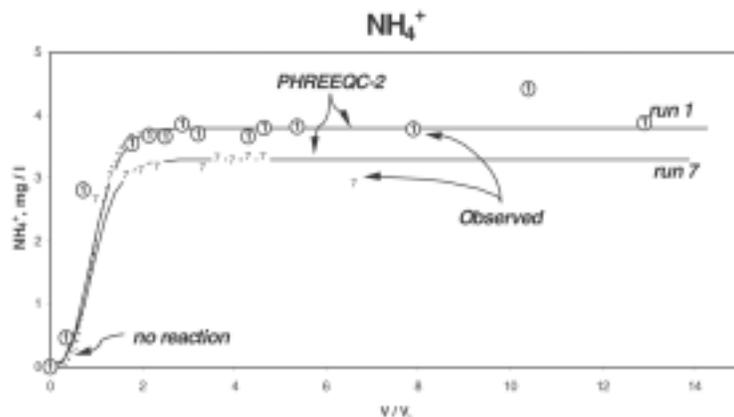

Figure 6. Observed and modeled ammonia concentrations in cyles 1 and 7 in Schuwacht.

Manganese

The Mn^{2+} ion sorbs both to clay minerals and to iron-oxyhydroxide, and the sediment's exchange capacity increases in proportion to the amount of iron-oxyhydroxide which precipitated in the previous runs. The increasing retardation associated with the increase of the sorption capacity is clearly visible in Figure 7 in the delayed increase of the Mn concentration in run 7 compared to run 1. The retardation is directly related to the number of sorption sites on the iron-oxyhydroxide precipitate which is discussed next. The model shows a reasonable match of the observed concentrations but tends to be less disperse.
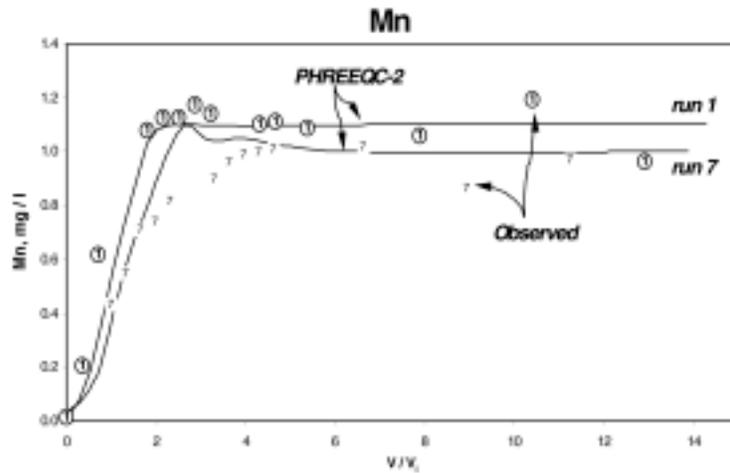
Figure 7. Observed and modeled manganese concentrations in cyles 1 and 7 in Schuwacht.

Iron

The iron concentrations during pumping in the first and seventh run are shown in Figure 8. Again, the end-concentration in groundwater fluctuated and was 6 and 5.2 mg Fe^{2+}/l for run 1 and 7, respectively. In the first run, a retardation of approximately 2.5 with respect to conservative behavior is indicated in Figure 8, which is close to what was calculated by hand before. The increased retardation in subsequent runs can be modeled if the sorption sites amount to 1.4 mol sites per mol Fe. This is quite high, Dzombak and Morel (1990) proposed 0.2 mol sites per mol ferrihydrite. Of course, the latter number is valid for laboratory conditions where the oxides are
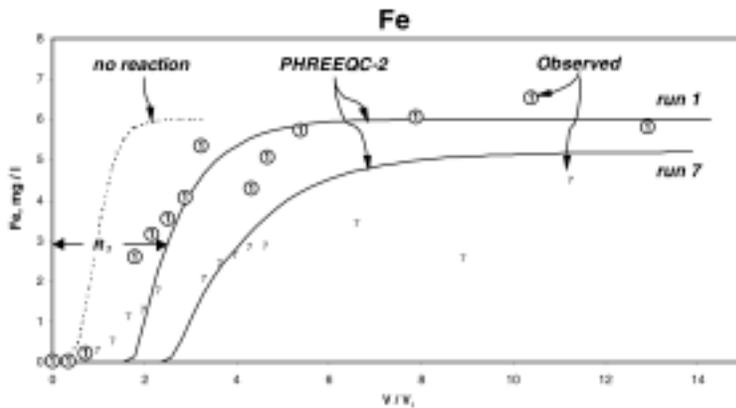

Figure 8. Observed and modeled iron concentrations in cyles 1 and 7 in Schuwacht.

prepared for more or less standardized experiments and aged and sometimes heated. It may be that during in situ iron removal, the precipitate forms a thin layer on existing surfaces of only a few atom layers thick, thus acquiring a specific surface area that is larger than in the laboratory preparates. Also, not all the sites are covered by ferrous iron, but phosphate and carbonate occupy more than 90% of the 1.4 mol sites per mol iron, which suggests that a complicated, mixed solid grows in the aquifer, and not a neat iron-oxyhydroxide with properties which remain invariant over months and for which sorption and desorption can be calculated with one and the same model. It is also probable that the efficiency increase will be less in later runs because the specific surface area diminishes when the precipitate grows in thickness and ripens out and incorporates and rejects various elements in a more crystalline solid. It can be noted here that in model runs with calcite equilibrium the pH is slightly higher and more iron is sorbed because the surface charge is more negative. The optimized number of sites then decreases to about 1.3 mol per mol iron. However, the modeled pH is somewhat higher than was measured.

The effect of sorption of HCO_3^- on ferrihydrite in the model also requires discussion. With the derived complexation constants, HCO_3^- was, together with phosphate, the dominant species on the weak sites of the ferrihydrite surface. Sorption had no effect on the groundwater concentrations of HCO_3^-, but the high HCO_3^- concentrations did affect the sorption of the other surface species, in particular of Fe^{2+} and PO_4^{3-}. Without sorption of HCO_3^-, the increased sorption of Fe^{2+} in run 7 compared to run 1 can be modeled with fewer sorption sites, 0.8 mol sites per mol Fe would be sufficient. However, even that number is high compared to the usual estimates for laboratory prepared ferrihydrite, and the formation of a mixed solid still seems the most plausible. The existing iron-oxyhydroxide in the aquifer was given an unreactivity factor of 3e-3, meaning that 300 ppm Fe initially amounted to (1.4 mol sites/mol Fe) $\times$ (300mg/kg / 56g/mol) $\times$ (ρ_b/ε = 6 kg/l) $\times$ 3e-3 = 0.135 mmol sites/l groundwater. The (un)reactivity factor was bracketed on the high end by retardation for iron in the first cycle, and on the low end by having sufficiently sorbed As available for desorption (discussed later).

The modeled concentration lines in Figure 8 are for a combination of a coarse sand (2/3 of aquifer thickness) and silty sand (1/3 of thickness). The higher initial exchange capacity of the silty sand increases the retardation, and smears out the concentration pattern. This does fit the observed slow increase to the final concentration in the first run, but the modeled pattern is too steep for the seventh run. It may be that the pattern is more spread out in the field because in the aquifer more layers exist with a different initial exchange capacity than in the simple two-units model. Such differences will lead to a faster initial breakthrough, and to a more retarded arrival of the

final concentration. However, it is also likely that kinetics of the Fe^{2+} oxidation and of the exchange and sorption reactions will play a role.

Phosphate

The 1.4 sorption sites per mol precipitated iron was determined by comparing the iron as well as the phosphate concentrations (Fig. 9). The sorption behavior of the two ions on ferrihydrite is intimately coupled. Sorption of HPO_4^{2-} and $H_2PO_4^-$ increases the negative charge of ferrihydrite, and stimulates sorption of Fe^{2+} (the surface of ferrihydrite would be positively charged at the pH of groundwater if phosphate would not be present). On the other hand, sorption of Fe^{2+} compensates the negative charge increase and thus tends to stimulate sorption of phosphate as well. Just as for iron, HCO_3^- has important effects in limiting sorption and in even more markedly influencing the concentration increases of phosphate. Without sorption of HCO_3^-, the modeled concentration increase of phosphate is much steeper as is shown in Figure 10, and the assumed two-layer structure of the model aquifer becomes quite conspicuous in two steps in the model lines. The stepwise character is a result of the steep sorption isotherm of phosphate on ferrihydrite when sorption of HCO_3^- is not in the model.

Arsenic

The arsenic concentration in pumped water varied from less than 2 µg As/l to 14 µg/l. The concentration pattern of As was different from the other elements and showed a marked concentration increase at the time that iron and phosphate arrived at the well (Fig. 11). The highest concentrations of 13-14 µg As/l were found in the first two cycles only, in later runs the concentrations decreased to less than 9 µg/l, although still showing a concentration jump when the iron and phosphate concentrations started to increase in the well. Only total arsenic concentrations were measured, but the modeled pattern in Figure 11 is the result of redox reactions of As(III) and As(V), of the different affinity of these species for ferrihydrite, and further marked by the displacement by phosphate. For an insight in the competing reactions which affect the behavior of As, it is helpful to calculate distribution coefficients for the groundwater quality at hand (first cycle in Table 3). The distribution coefficients relate the concentration sorbed to solute, and are given in undimensionalized form in Table 4.

Inspecting Table 4, it can be noted that arsenite is much less sorbed than arsenate in groundwater without phosphate. However, in the presence of PO_4^{3-} the sorption of arsenate is diminished to a very small quantity due to negative charging of the ferrihydrite surface. The effect is greater for arsenate than for arsenite because arsenate is sorbed as a negative species, while arsenite forms a neutral surface complex. The HCO_3^- surface complex also is mainly neutral, and the ion floods the weak sites of ferrihydrite and
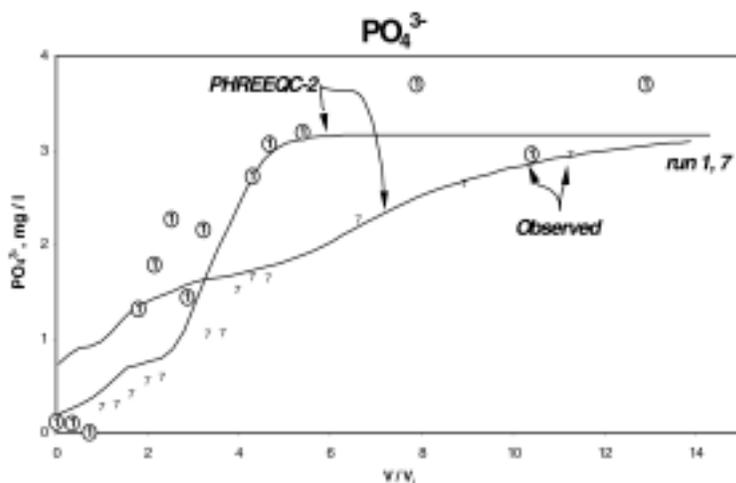
Figure 9. Observed and modeled phosphate concentrations in cyles 1 and 7 in Schuwacht.
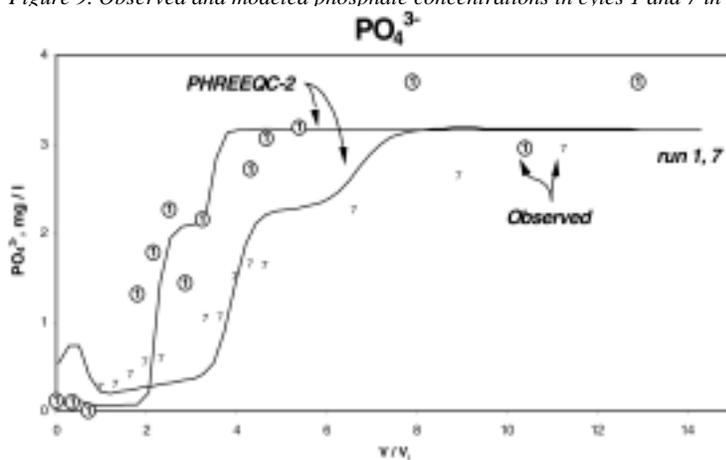

Figure 10. Observed and modeled phosphate concentrations in cyles 1 and 7 in Schuwacht, without sorption of HCO_3^- on ferrihydrite.

displaces arsenite while the effect on arsenate is somewhat less. On the other hand, sorption of Fe^{2+} charges the surface positively, and enhances sorption of arsenate, while it merely competes for sorption sites with arsenite. The smaller distribution coefficient for groundwater compared to injected water, is entirely due to the presence of more phosphate and HCO_3^- in groundwater.

Now, the effect of injection of oxidized water is that As(III) is oxidized, and since As(V) is sorbed stronger than As(III), dissolved concentrations would diminish. However, when PO_4^{3-} contacts the surface to which As(V)
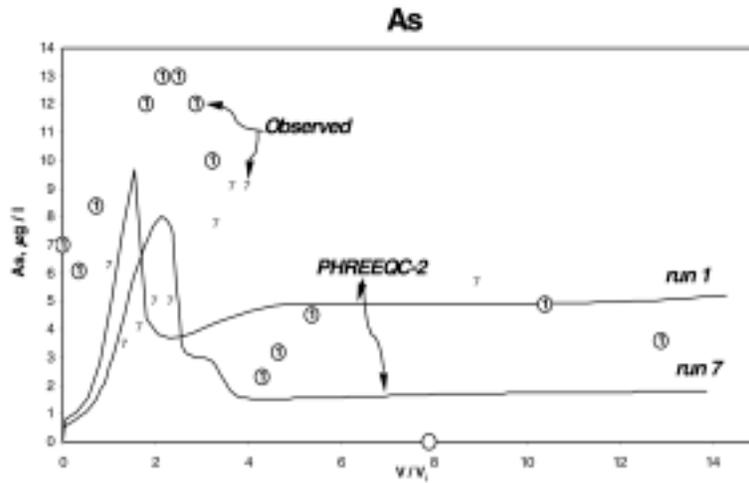
Figure 11. Observed and modeled arsenic concentrations in cyles 1 and 7 in Schuwacht.

Table 3. Composition of native groundwater and injected waters, in pH units and mg/l. Temperature is 10°C.

	Groundwater		*Injected water*	
	Cycle 1-3	Cycle 4-7	Cycle 1-2	Cycle 3-7
pH	7.1	7.1	7.4	7.65
Na	77.3	77.3	65.5	65.5
K	5.3	4.8	3.6	3.6
Mg	13.1	12.2	11.5	11.5
Ca	93	87	83	83
NH_4^+	3.8	3.3	0.01	0.01
Fe	6.0	5.2	0	0
Mn	1.1	1.0	0	0
Cl	134	137	124	124
HCO_3^-	308	260	214	201
SO_4	43.4	51.0	44.0	44.0
PO_4	3.16	3.16	0.1	0.1
As (µg/l)	10	5	0	0

is attached, it desorbs As, as indicated by the low distribution coefficient (Table 4). According to the model calculations, PO_4^{3-} displaces As in the form of a wave which arrives in the well just before the increase of the phosphate concentration. As soon as Fe^{2+} arrives, As(V) is reduced to As(III) which is less affected by PO_4^{3-} and sorbs again in agreement with the higher distribution coefficient. To model the concentration wave of arsenic, sufficient As(III) must be present in the system. Thus, in the first run the number of sorption sites on iron-oxyhydroxide had to be adequate and this

bracketed the (un)reactivity factor for already present iron-oxyhydroxide in the aquifer. Also, the surface complexation constant for H_3AsO_3 was increased threefold to obtain sufficiently sorbed arsenic.

Table 4. Model distribution coefficients for As, (mol adsorbed/l) / (mol solute/l), on 1 mmol ferrihydrite for groundwater at Schuwacht.

	As(III)	As(V)
Fe, Alk, PO$_4$, all 0 mg/l	22	211
6 mg Fe/l[1]	18	234
3.16 mg PO$_4$/l[1]	6	2
308 mg HCO$_3$/l[1]	6	36
Fe, Alk, PO$_4$ all at groundw. conc.[1]	4	1
Injected water[1]	12	53

[1]Groundwater concentration from Table 3

The modeled pattern in Figure 11 shows the observed concentration trends, but, clearly, it does not match the details. Notably, the predicted As peaks arrive too early and they are too small. The column experiments of Isenbeck-Schrˆter (1995) and Darland and Inskeep (1997) required kinetic reactions for Freundlich or Langmuir sorption isotherms for As, but a kinetic model appears to spread out the As concentrations in Figure 11 only, and it does not shift the position of the peak to later arrival times. Therefore, other reactions might explain the discrepancy.

First, it is remarkable that the As concentration was quite high already when injected water was backpumped. It may be that As was sorbed to colloidal iron-oxyhydroxide particles formed during oxidation, but were too small to be removed by filtration over 0.45 µm before analysis. This mechanism was suggested by Rott et al. (1996) who observed similar As peaks during the first cycles of an in situ iron removal system. When samples were analyzed from a later cycle in Schuwacht, the As concentrations had decreased to about 2 µg As/l and they were similar in unfiltered and 0.1 µm filtered subsamples. Thus, sorption to colloidal iron cannot be ruled out as a mechanism and it should be investigated thoroughly in the incipient cycles of another system.

Second, the combined presence of Fe^{2+} and Mn^{2+} in groundwater, and precipitation of both Mn-oxides and Fe-oxides would lead to separation in space of the precipitates, with Fe^{2+} reducing the Mn-oxides (Postma and Appelo, 2000). This may have special, but as yet not quantified effects on the behavior of As.

Third, the surface complexation model of Dzombak and Morel (1990) is based on data published by Pierce and Moore (1982) and is excellent for

calculating laboratory experiments with As by Wilkie and Hering (1996) and Manning and Goldberg (1996). The data of Manning and Goldberg only require a small adaptation of the ionic strength to use the double layer model and to arrive at a similar potential/charge relation for ferrihydrite as for the constant capacity model which they applied. These authors investigated competition of SO_4^{2-} and PO_4^{3-} for sorption of As. However, the multicomponent effects of a natural groundwater are still to be verified and a column experiment with well defined conditions and water qualities is highly desirable for elucidating the combined effects of the various processes on As during in situ iron removal.

5.   SUMMARY

The principles of in situ iron removal from groundwater were explained in simple terms, based on the reaction of sorbed ferrous iron in the aquifer. The efficiency of an in situ iron removal system was defined as the ratio of the volume of groundwater pumped to the volume of oxygenated water injected. For the easy case of sharp fronts without dispersion or smearing by kinetics, the efficiency is given by the ratio of the retardation of Fe^{2+} over the retardation of O_2, $E = V_{gw}/V_{inj} = R_{Fe}/R_{O_2}$. A specific case of in situ iron removal in the Netherlands was discussed, showing many of the details of in situ iron removal common to these systems. The features are connected with exchange and sorption reactions in the aquifer. Sorption for ammonium was small and identical for all cycles. Retardation of Mn^{2+}, Fe^{2+} and PO_4^{3-} increased in successive cycles due to sorption to the iron-oxyhydroxide which was precipitated in the previous cycles. The concentration patterns of these elements could be modeled well with known reactions. Arsenic showed a complicated behavior with initial concentration jumps which appear to be related to redox transitions and displacement by PO_4^{3-}. A relatively high sorption capacity of the freshly precipitated ferrihydrite suggests that the precipitate in the aquifer is a mixed solid of Fe, P and C, rather than a neat iron-oxyhydroxide to which Fe^{2+} and other elements are sorbed.

ACKNOWLEDGEMENTS

Appelo, C. A. J., Drijver, B., Hekkenberg, R., and De Jonge, M., 1999, Modeling in situ iron removal from ground water: Ground Water, v. 37, p. 811-817.

Appelo, C. A. J., and Postma, D., 1993, Geochemistry, groundwater and pollution: Rotterdam, Balkema, 536 p.

Appelo, C. A. J., Van der Weiden, M. J. J., Tournassat, C., and Charlet, L., 2002, Surface complexation of ferrous iron and carbonate on ferrihydrite and the mobilization of arsenic: Environmental Science & Technology, v. 36, p. 3096-3103.

Benjamin, M. M., Sletten, R. S., Bailey, R. P., and Bennett, T., 1996, Sorption and filtration of metals using iron-oxide coated sand: Water Research, v. 30, p. 2609-2620.

Darland, J. E., and Inskeep, W. P., 1997, Effects of pore water velocity on the transport of arsenate: Environmental Science & Technology, v. 31, p. 704-709.

Davis, J. A., Coston, J. A., Kent, D. B., and Fuller, C. C., 1998, Application of the surface complexation concept to complex mineral assemblages: Environmental Science & Technology, v. 32, p. 2820-2828.

Dzombak, D., and Morel, F., 1990, Surface Complexation Modeling: Hydrous Ferric Oxide: New York, Wiley, 393 p.

Eick, M. J., Peak, J. D., Brady, P. V., and Pesek, J. D., 1999, Kinetics of lead adsorption/desorption on goethite: Residence time effect: Soil Science, v. 42, p. 28-39.

Fuller, C. C., Davis, J. A., and Waychunas, G. A., 1993, Surface-chemistry of ferrihydrite. 2. Kinetics of arsenate adsorption and coprecipitation: Geochimica et Cosmochimica Acta, v. 57, p. 2271-2282.

Gerth, J., Bruemmer, G. W., and Tiller, K. G., 1993, Retention of Ni, Zn and Cd by Si-associated goethite: Z. Pflanzenern. Bodenk, v. 156, p. 123-129.

Hallberg, R. O., and Martinell, R., 1976, Vyredox - in situ purification of groundwater: Ground Water, v. 14, p. 88-93.

Isenbeck-Schrˆter, M., 1995, Transport conditions of heavy metals and oxoanions - column experiments and their modeling: Ber. Geowissenschaften, v. 67, University of Bremen, Germany, 182 p.(in German).

Kent, D. B., Abrams, R. H., Davis, J. A., Coston, J. A., and LeBlanc, D. R., 2000, Modeling the influence of variable pH on the transport of zinc in a contaminated aquifer using semiempirical surface complexation models: Water Resources Research, v. 36, p. 3411-3425.

Liger, E., Charlet, L., and Van Cappellen, P., 1999, Surface catalysis of Uranium(VI) reduction by iron(II): Geochimica et Cosmochimica Acta, v. 63, p. 2939-2955.

Manning, B. A., and Goldberg, S., 1996, Modeling competitive adsorption of arsenate with phophate and molybdate on oxide minerals: Soil Science Society of America Journal, v. 44, p. 609-623.

Mathur, S. S., 1995, Development of a database for ion sorption on goethite using surface complexation modeling [MSc thesis]: Carnegie Mellon Univ., 178 p.

McKenzie, R., 1980, The adsorption of lead and other heavy metals on oxides of Mn and Fe.: Australian Journal of Soil Research, v. 18, p. 61-73.

Meyerhoff, R., 1996, Planning and application of in situ iron and manganese treatment of groundwater: Ber. Siedlungswasserbau, v. 139, University of Stuttgart, Germany. (in German).

Nesbitt, H.W., Muir, I.J. and Pratt, A.R., 1995. Oxidation of arsenopyrite by air and air-saturated, distilled water, and implications for mechanism of oxidation: Geochimica et Cosmochimica Acta, v. 59, p. 1773-1786.

Parkhurst, D. L., and Appelo, C. A. J., 1999, User's guide to PHREEQC (version 2): U.S. Geological Survey Water-Resources Investigations Report 99-4259, 312 p.

Pierce, M. L., and Moore, C. B., 1982, Adsorption of arsenite and arsenate on amorphous iron hydroxide: Water Research, v. 16, p. 1247-1253.

Postma, D., and Appelo, C. A. J., 2000, Reduction of Mn-oxides by ferrous iron in a flow system: Column experiment and reactive transport modeling: Geochimica et Cosmochimica Acta, v. 64, p. 1237-1247.

Rott, U., and Lamberth, B., 1993, Groundwater clean up by in situ treatment of nitrate, iron and manganese: Water Supply 11, p. 143-156.

Rott, U., Meyerhoff, R., and Bauer, T., 1996, In situ treatment of groundwater with increased concentrations of iron, manganese and arsenic: Wasser-Abwasser, v. 137, p. 358-363 (in German).

Runkel, R. L., Kimball, B. A., McKnight, D. M., and Bencala, K. E., 1999, Reactive solute transport in streams: a surface complexation approach for trace metal sorption: Water Resources Research, v. 35, p. 3829-3840.

Stollenwerk, K. G., 1998, Molybdate transport in a chemically complex aquifer: Field measurements compared with solute transport model predictions: Water Resources Research, v. 34, p. 2727-2740.

Van Beek, C. G. E. M., 1980, A model for the induced removal of iron and manganese from groundwater in the aquifer, *in* 3rd Water-Rock Interaction Symposium, Edmonton, Canada, p. 29-31.

Van Geen, A., Robertson, A. P., and Leckie, J. O., 1994, Complexation of carbonate species at the goethite surface: implications for adsorption of metal ions in natural waters: Geochimica et Cosmochimica Acta, v. 58, p. 2073-2086.

Waychunas, G. A., Rea, B. A., Fuller, C. C., and Davis, J. A., 1993, Surface chemistry of ferrihydrite: Part 1. EXAFS studies of the geometry of

coprecipitated and adsorbed arsenate: Geochimica et Cosmochimica
Acta, v. 57, p. 2251-2269.

Wilkie, J. A., and Hering, J. G., 1996, Adsorption of arsenic onto hydrous
ferric oxide: effects of adsorbate/adsorbent ratios and co-occurring
solutes: Colloids and Surfaces A, v. 107, p. 97-110.

Zachara, J. M., Girvin, D. C., Schmidt, R. L., and Resch, C. T., 1987,
Chromate adsorption on amorphous iron oxyhydroxide in the
presence of major groundwater ions: Environmental Science &
Technology, v. 21, p. 589-594.